ISSN 0869-5938, Stratigraphy and Geological Correlation, 2006, Vol. 14, No. 5, pp. 463–474. © MAIK "Nauka/Interperiodica" (Russia), 2006.
Original Russian Text © A.M. Larin, E.B. Sal'nikova, A.B. Kotov, L.B. Makar'ev, S.Z. Yakovleva, V.P. Kovach, 2006, published in Stratigrafiya. Geologicheskaya Korrelyatsiya, 2006, Vol. 14, No. 5, pp. 3–15.

Early Proterozoic Syn- and Postcollision Granites in the Northern Part of the Baikal Fold Area

A. M. Larin[a], E. B. Sal'nikova[a], A. B. Kotov[a], L. B. Makar'ev[b], S. Z. Yakovleva[a], and V. P. Kovach[a]

[a]*Institute of Precambrian Geology and Geochronology, Russian Academy of Sciences, St. Petersburg, Russia*
[b]*All-Russia Research Institute of Geology, St. Petersburg, Russia*

Received June 22, 2005

Abstract—Early Proterozoic granitoids are of a limited occurrence in the Baikal fold area being confined here exclusively to an arcuate belt delineating the outer contour of Baikalides, where rocks of the Early Precambrian basement are exposed. Geochronological and geochemical study of the Kevakta granite massif and Nichatka complex showed that their origin was related with different stages of geological evolution of the Baikal fold area that progressed in diverse geodynamic environments. The Nichatka complex of syncollision granites was emplaced 1908 ± 5 Ma ago, when the Aldan–Olekma microplate collided with the Nechera terrane. Granites of the Kevakta massif (1846 ± 8 Ma) belong to the South Siberian postcollision magmatic belt that developed since ~1.9 Ga during successive accretion of microplates, continental blocks and island arcs to the Siberian craton. In age and other characteristics, these granites sharply differ from granitoids of the Chuya complex they have been formerly attributed to. Accordingly, it is suggested to divide the former association of granitoids into the Chuya complex proper of diorite–granodiorite association ~2.02 Ga old (Neymark et al., 1998) with geochemical characteristics of island-arc granitoids and the Chuya–Kodar complex of postcollision S-type granitoids 1.85 Ga old. The Early Proterozoic evolution of the Baikal fold area and junction zone with Aldan shield lasted about 170 m.y. that is comparable with development periods of analogous structures in other regions of the world.

DOI: 10.1134/S0869593806050017

Key words: Early Proterozoic, syn- and postcollision granites, Baikal fold area, geochronology, South Siberian magmatic belt.

INTRODUCTION

The Baikal fold area of Riphean and Paleozoic rock complexes is part of the Central Asian giant foldbelt. The Early Proterozoic granitoids are of a limited occurrence in that system being confined there exclusively to an arcuate belt delineating the outer contour of Baikalides, where rocks of the Early Precambrian basement are exposed (Fig. 1). These are granitoids of the Chuya (or Chuya–Kodar), Irel, Abchad, Tatarnik, Kocherikov, Primorskii, and Nichatka complexes. Recent geochronological and geochemical data elucidating the successive formation and tectonic typification of these granitoids are still insufficient for geodynamic modeling of Precambrian magmatic evolution of the Baikal fold area. In view of this situation, we carried out geochronological and geochemical study of granitoids from the Kevakta massif and Nichatka complex (Fig. 1). Age and tectonic position of these granitoids can be of key significance for understanding the origin and evolution of the Early Proterozoic granitoid magmatism in the region under consideration.

GEOLOGICAL SITUATION

The Kevakta massif spans a greater part of the Tonod basement block in the north of the Baikal fold area. This relatively large massif extending in sublatitudinal direction has intruded the Early Proterozoic supracrustal rocks of the Mikhailovka and Abaza formations and is overlain by the Riphean high-Al metasedimentary rocks of the Purpol Formation of the Bodaibo–Patom zone. Besides, granites of the Kevakta massif are crosscut by minor subvolcanic bodies of spherulitic granite-porphyry of the Yazov complex, which are 726 ± 4 Ma old (Larin et al., 1998). The Kevakta massif has been commonly regarded as a unit of the Chuya complex that includes granitoids dated at 2020 ± 12 Ma in synonymous basement block (Neymark et al., 1998). Geological and geochemical data imply however that granitoids of this complex are very different in the Chuya and Tonod basement blocks (Neymark et al., 1998), and it is hardly reasonable to attribute them to a single complex (Larin et al., 2003a).

Small intrusive bodies of "black-feldspar" two-mica pegmatoid granite, which are attributed to the Nichatka complex, are concentrated almost exclusively in the junction zone of the Baikal fold area (Nechera base-

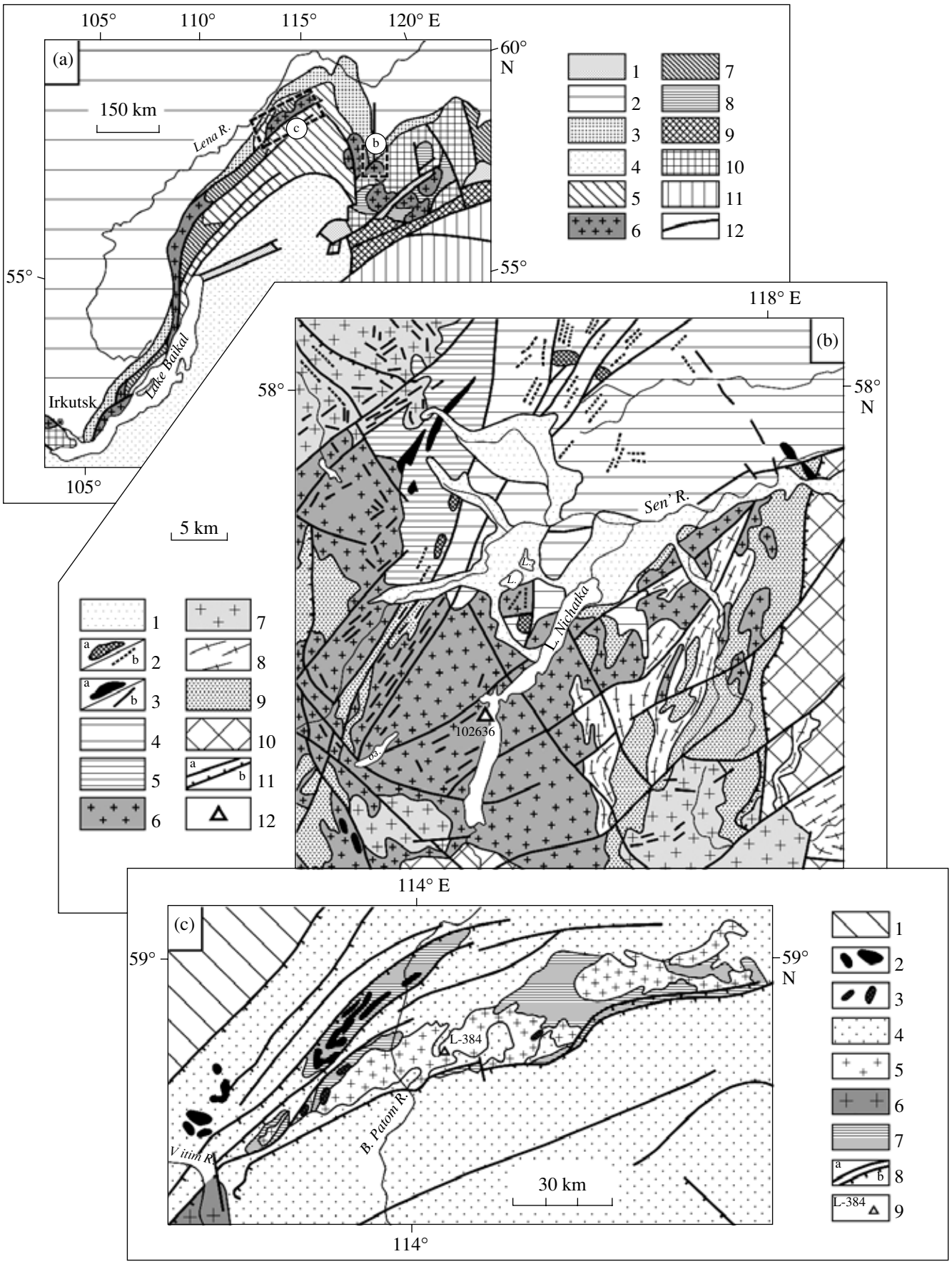
105°
110°
115°
120° E
(a)
60° N
150 km
Lena R.
c
b
1
2
3
4
5
6
7
8
9
10
11
12
55°
55°
Irkutsk
Lake Baikal
105°
118° E
(b)
58°
58° N
Sen' R.
L.
L. Nichatka
102636
5 km
1
2
3
4
5
6
7
8
9
10
11
12
114° E
(c)
59°
59° N
L-384
B. Patom R.
Vitim R.
30 km
1
2
3
4
5
6
7
8
9
L-384
114°

Fig. 1. Tectonic scheme of the South Siberian platform (a) and maps illustrating geological structure of areas with collision-related granitoids of the Nichatka (b) and Chuya–Kodar (c) complexes. Symbols in Fig. 1a: (1) Mesozoic and Cenozoic rifts and superimposed troughs; (2) sedimentary cover of Siberian platform; (3) Riphean pericratonic troughs; (4) Central Asian foldbelt; (5) Riphean folded rocks on Early Precambrian basement; (6) Early Proterozoic syn- and postcollision igneous rocks; (7) Early Proterozoic foldbelts; (8) Early Proterozoic epicratonic basins; (9) Early Proterozoic suture zone (Cis-Stanovoi belt of high-P granulites); (10) Archean blocks of Siberian platform margin; (11) Archean–Early Proterozoic Dzhugdzhur–Stanovoi foldbelt; (12) major faults. Symbols in Fig. 1b: (1) Quaternary deposits; (2) Mesozoic alkaline intrusions (a) and dikes(b) of the Murun complex; (3) dolerite intrusions (a) and diabase dikes (b) of the Riphean Doros complex (R_3); (4) sedimentary rocks of the Riphean Sen Formation (R_{2-3}); sedimentary rocks of Riphean Balaganakh and Bol'shoi Tor groups (R_2) and Purpol Formation (R_1); (6) Nichatka complex of the Early Proterozoic granites; (7) undivided granites of the Early Proterozoic; (8) Kuanda complex of Early Proterozoic gneissic and migmatized granites; (9) Lower Proterozoic metasedimentary rocks in the Udokan-type basins; (10) tonalites, gneissic granites, granulites and supracrustal rocks of the Chara–Olekma tectonic block of the Aldan shield (AR); (11) normal (a) and thrust (b) faults; (12) sampling site of geochronological study; L—lake. Symbols in Fig. 1c: (1) sedimentary cover of Siberian platform; (2) diabase dikes and sills of the Late Riphean Chai complex; (3) granite-porphyries of the Late Riphean Yazov complex; (4) Late Riphean metamorphic rocks of the Bodaibo–Patom zone; (5) Early Proterozoic granites of the Chuya–Kodar complex; (6) Chuya complex of Early Proterozoic granitoids; (7) Mikhailovka and Abaza formations of Early Proterozoic supracrustal rocks; (8) normal(a) and thrust (b) faults; (9) sampling site of geochronological study.

ment block) and Aldan shield (western area of the Chara–Olekma block). These bodies have intruded rocks of the Udokan Group (2180 ± 50 Ma, Berezhnaya et al., 1988) and undivided granitoids of the Early Proterozoic, being overlain by Riphean deposits of the Baikal pericratonic trough (Figs. 1a, 1b). Within the Zhuin fault zone, granites of the Nichatka complex are crosscut by Riphean dikes of the Doros complex, which strike predominantly in northeastern direction.

ANALYTICAL METHODS

Chemical composition of studied rocks is determined by the XRF method, and concentrations of trace elements are measured either by the same (Rb, Sr, Y, Zr, Nb, Pb, Th, Ba, Cr, Co, Ni, V) or by the ICP MS method (REE, Li, Be, Sc, Cu, Zn, Ga, Y, Nb, Cs, Hf, Ta, Th, U) with the relative uncertainty of 5–10%.

Standard separation method in heavy liquids has been applied to extract accessory zircons from rock samples. The U–Pb dating is performed for zircon fractions 0.43 to 0.79 mg in weight and for lesser amount of hand-picked grains (2–30). Optical and cathodoluminescence microscopy is applied to study inner structure of individual zircon grains. Surface contamination of zircon crystals selected for geochronological analysis has been cleaned up successively in alcohol, acetone and 1M HNO_3. After each step, crystals have been washed in specially purified water. The modified Krogh's method (Krogh, 1973) has been used to decompose crystals and to extract Pb and U. Total blank was not greater than 30 pg for Pb and 5 pg for U. Isotopic composition is determined in static or jumping mode on multicollector mass spectrometer Finnigan MAT 261 equipped with a secondary electron multiplier (discrimination coefficient of multiplier is 0.32 ± 0.11 for Pb).

Experimental data are processed using programs PbDAT (Ludwig, 1991) and ISOPLOT (Ludwig, 1999). Standard U decay constants (Steiger and Jager, 1976) are used to calculate age values. Correction for common lead is consistent with that accepted in model by Stacey and Kramers (1975). All uncertainties are quoted at 2σ level.

GEOCHEMICAL CHARACTERISTICS OF GRANITOIDS

Data on chemical composition and concentrations of REE and other trace elements in granitoids of the Chuya and Nichatka complexes are presented in Tables 1 and 2. In the Chuya basement block, granitoids of synonymous complex are represented mostly by dominant diorites, quartz-diorites, and subordinate granodiorites. These rocks with $Na_2O/K_2O > 1$ belong to calc-alkaline and calcic series. Prevalent among them are low-Al rocks with moderate index FeO*/FeO* + MgO = 0.65–0.89. The HFSE and LILE

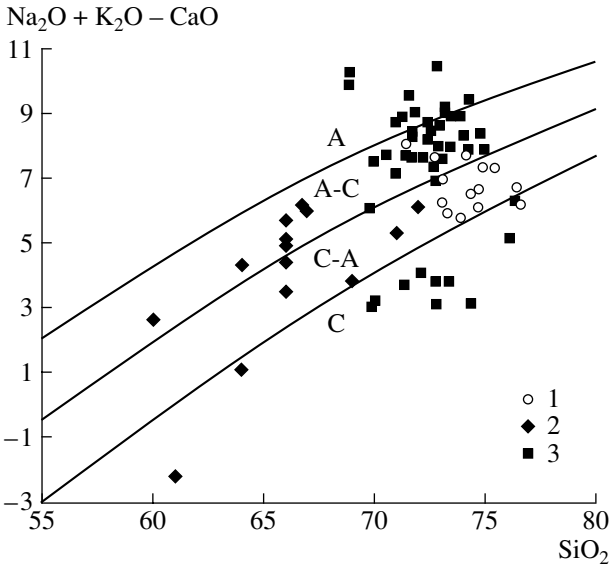

Fig. 2. Granitoids of the Chuya–Kodar (1, Kevakta massif), Chuya (2) and Nichatka (3) complexes in ($Na_2O + K_2O – CaO – SiO_2$ diagram with fields (after Frost et al., 2001) of alkaline (A), alkali-calcic (A-C), calc-alkaline (C-A) and calcic (C) rocks.

Table 1. Chemical composition of representative samples of Early Proterozoic granitoid from the Baikal fold area

Components	Chuya–Kodar complex (Kevakta massif)				Chuya complex			Nichatka complex		
	L-290*	L-384	L-383	L-385	SH-58	3110/29	35-89	10263-6	10075	10176-1
	CBG	CBG	CBG	FBG	T	B-AGD	B-AGD	PG	PG	LG
SiO_2	73.06	73.02	73.34	75.44	70.00	66.00	66.80	68.90	73.01	71.85
TiO_2	0.22	0.30	0.31	0.12	0.33	0.44	0.32	0.29	0.06	0.09
Al_2O_3	13.85	13.76	13.28	12.68	15.40	16.50	15.40	15.91	14.99	14.73
Fe_2O_3	2.75	3.34	3.10	2.37	3.40	3.80	3.40	1.56	0.78	2.45
FeO										
MnO	0.03	<0.02	0.04	0.04	0.043	0.062	0.073	<0.01	<0.01	0.04
MgO	0.22	0.31	1.48	<0.2	1.40	1.60	1.60	1.10	0.27	0.28
CaO	0.97	0.31	0.34	0.43	2.90	3.20	2.70	0.54	0.82	0.48
Na_2O	2.42	2.00	1.82	2.58	5.00	4.90	5.30	2.76	2.89	3.29
K_2O	4.78	5.81	4.42	5.14	1.10	2.70	3.50	7.63	6.54	6.18
P_2O_5	0.20	0.16	0.12	0.14	0.12	0.25	0.19	<0.05	0.06	0.06
H_2O										
L.O.I.	0.99	<0.5	1.24	0.52	0.79	0.68	0.43	1.05	0.50	0.62
F	0.096	0.19	0.11	0.22						
Li	50	120	94	100		2.6		3.7		17.5
Rb	199	315	285	379	35	43	117	156	131	309
Sr	113	62	54	36	474	903	919	451	182	92
Y	22	27	35	21	7	15	9	8	6	39
Zr	129	136	160	97	175	156	106	19	52	114
Hf	1.03	2.44				2.10		0.17		3.28
Nb	9	13	19	19	6	14	4	10	<5	8
Ta	0.64	0.76				0.22		0.55		0.54
Pb	24	21	21	26	12	9	15	59	61	46
Th	16.0	23.0	29.0	20.0	4	4	1	6	<5	40
U	1.5	3	6	13		0.6		0.2		4.6
Ba	1255	756	748	418	598	1745	519	4802	1018	609
Cr	47		57	50	38	45	54	4.7		6.0
Ni	7	11	20	10	7	12	11	4.8		4.3
Co	<10	<10	<10	<10	11	3	2	1.7		1.6
V	<10	<10	<10	<10	36	37	60	<10	<10	<10
Zn	41.6	45.3				35.7		28.4		26.0

Note: (B-AGD) biotite–amphibole granodiorite; (CBG) coarse-grained biotite granite; (FBG) fine-grained biotite granite; (T) trondhjemite; (PG) pegmatoid granite; (LG) leucogranite; (L-290* etc.) sample numbers.

concentrations in granitoids under consideration are relatively low, except for Ba and Sr. In discrimination diagrams, relevant data points plot in the field of volcanic arc granitoids (Fig. 4). REE spectra of the Chuya complex granitoids (Fig. 3) are highly fractionated ($[La/Yb]_N = 29.8$, $[La]_N = 80.2$, $[Yb]_N = 2.7$), lacking Eu anomaly (Eu/Eu* = 0.99). A specific feature of patterns in Fig. 3 is their concave character in the HREE interval that is typical of magmatic arc granitoids and TTG association.

Biotite and biotite-muscovite, sometimes tourmaline granites of the Kevakta massif are typical representatives of subalkaline K-granites of S-type (Larin et al., 2003a). These are rocks of calc-alkaline and alkali-calcic series (Fig. 2), which are represented mostly by high-Al granites (A/CNK = 0.97–1.58) relatively enriched in Fe (FeO*/FeO* +MgO = 0.77–0.96). Concentrations of incompatible elements in the Kevakta granites are at a moderate level, except for the relative enrichment in Rb (200–300 ppm), Li (50–120 ppm)

Table 2. REE concentrations in the Early Proterozoic granitoids of the Baikal fold area

Components	Nichatka complex		Chuya–Kodar complex		Chuya complex
	10263-6	10176-1	L-290	L-384	3110/29
La	15.07	50.56	30.8	15.3	29.4
Ce	24.21	116.60	64	59	65
Pr	2.11	12.76	7.34	4.18	7.37
Nd	7.37	48.42	27.09	15.65	26.41
Sm	1.02	8.75	5.41	3.83	4.28
Eu	2.22	0.60	1.13	0.51	1.16
Gd	0.75	6.25	4.36	3.67	2.96
Tb	0.07	0.87	0.67	0.66	0.35
Dy	0.29	5.54	3.09	3.66	1.47
Ho	0.05	1.36	0.54	0.74	0.28
Er	0.11	4.58	1.19	1.86	0.70
Tm	0.01	0.76	0.15	0.27	0.10
Yb	0.05	5.23	0.86	1.63	0.67
Lu	0.01	0.68	0.12	0.20	0.08
$[La/Yb]_N$	191.2	6.53	24.16	6.36	29.75
$[La/Sm]_N$	9.32	3.64	3.58	2.52	4.32
$[Gd/Yb]_N$	11.42	0.97	4.11	1.82	3.59
Eu/Eu*	7.75	0.25	0.71	0.41	0.99

and F (0.1–0.22%). Being also enriched in LREE ($[La]_N$ = 83.8, $[La/Yb]_N$ = 24.2), these granites show distinct Eu anomalies (Eu/Eu* = 0.41–0.27, Fig. 3). In tectono-magmatic discrimination diagrams (Fig. 4), data points characterizing granites of the Kevakta massif plot in the field of postcollision granitoids.

Granites of the Nichatka complex are of subalkaline type in general. However, proportions of alkalies in the rocks are very variable, and some rock varieties correspond in composition to alkaline and calcic series, although data points of these granitoids mostly plot in the alkali-calc field of (Na_2O + K_2O–CaO)–SiO_2 diagram (Fig. 2). According to high saturation with alumina (1.04–1.69), variable saturation with iron (0.45–0.98) and all other peculiarities, rocks of the complex are close to S-type granitoids. In general, they are depleted in many incompatible elements despite highly variable trace-element concentrations. Pegmatoid varieties of the Nichatka granitoids are enriched in K, Ba and Sr, being considerably depleted in HFSE and REE. The last group of elements is somewhat enriched in LREE but extremely depleted in HREE ($[La/Yb]_N$ = 192; $[La]_N$ = 41.1; $[Yb]_N$ = 0.21), while positive Eu anomaly characteristic of the rocks is correlative with high Ba and Sr but low HREE and Zr concentrations. In our opinion, high Ba, Sr and Eu concentrations may reflect presence of cumulate feldspars, and fractionation of zircon or garnet can be responsible for depletion in HREE. In late leucogranites of the Nichatka complex, concentrations of many incompatible elements increase parallel to decreasing Ba, Sr and K content. The REE, especially HREE concentration growth is accompanied by a higher fractionation degree of these elements ($[La/Yb]_N$ = 6.5; $[La]_N$ = 137.8; $[Yb]_N$ = 17.8) and by emergence of negative Eu anomaly (Eu/Eu* = 0.25). The last effect and decline of Ba, Sr and K concentrations are most likely related to fractionation of feldspars; the increase of REE (HREE espe-

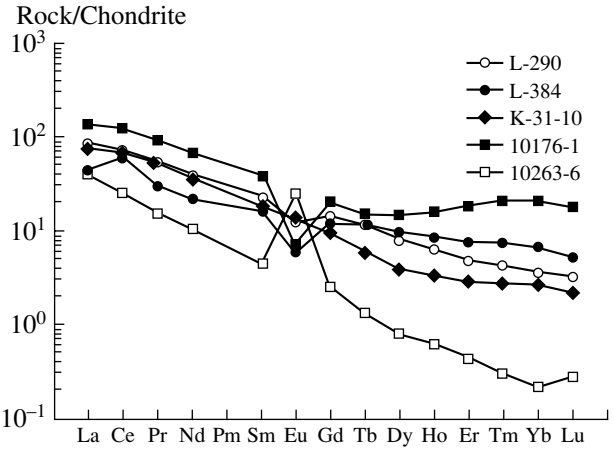

Fig. 3. Chondrite-normalized REE patterns of granitoids from the Kevakta massif of the Chuya–Kodar complex (L-290, L-384) and from the Chuya (K-31-10) and Nichatka (10176-1, 10263-6) complexes.

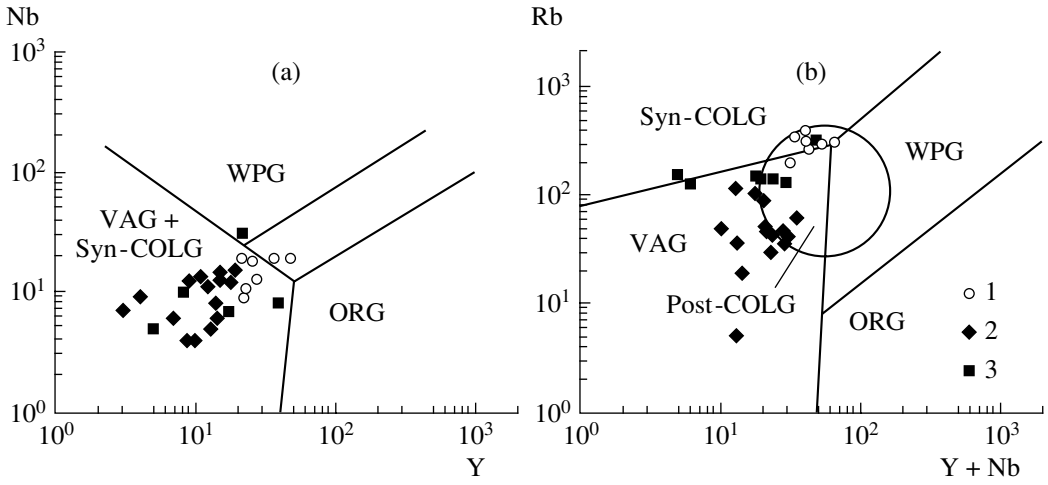

Fig. 4. Studied granitoids in geochemical discrimination diagrams (a) Y–Nb and (b) Rb–(Y + Nb) with fields of within-plate (WPG), orogenic (ORG), volcanic-arc (VAG) syncollision (syn-COLG) and postcollision (post-COLG) granitoids (after Pearce et al., 1984; Pearce, 1996; symbols as in Fig. 2).

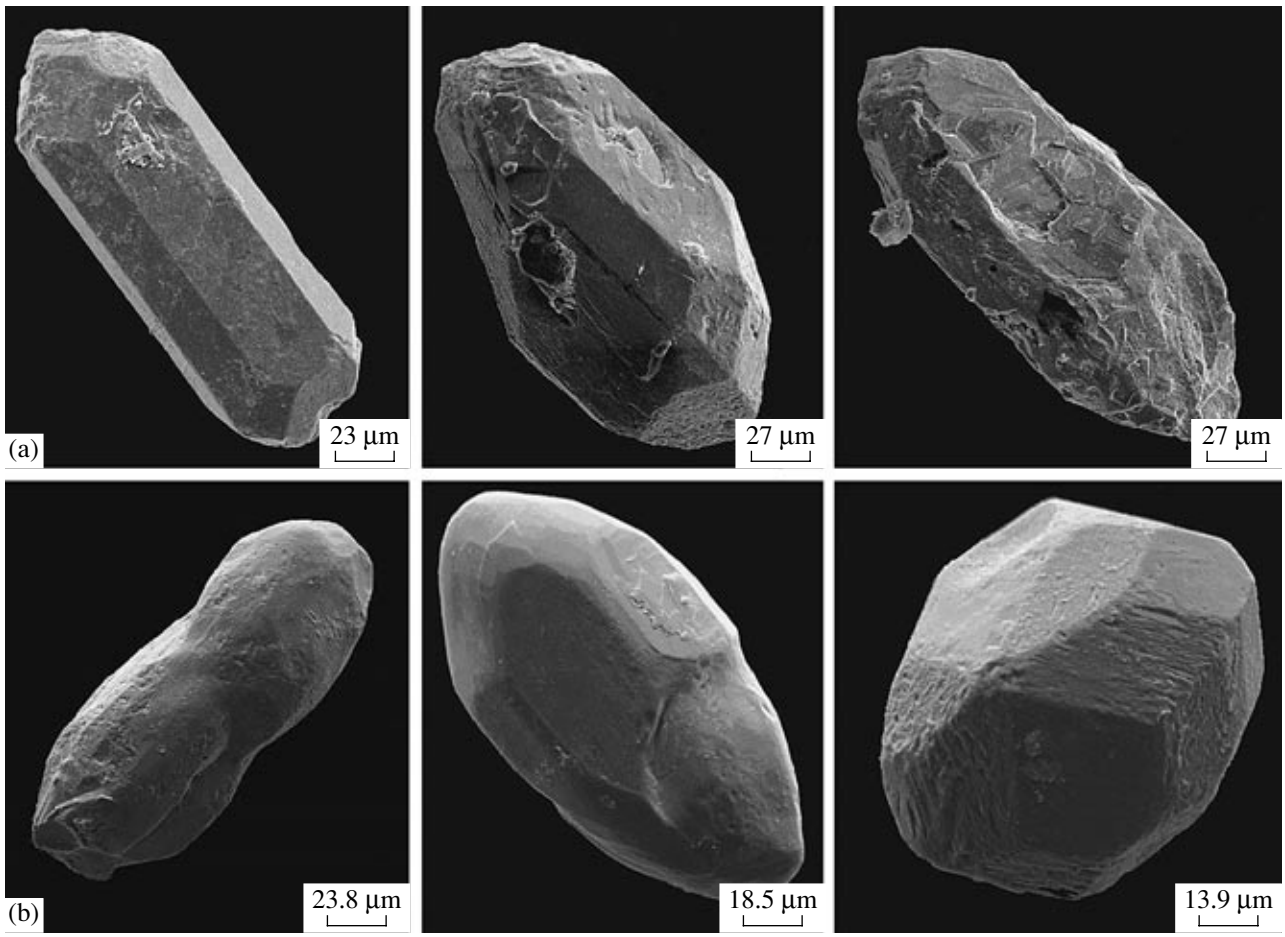

Fig. 5. Microphotographs of zircon crystals from granites of the Kevakta massif, Sample L-384 (a), and Nichatka complex, Sample 10263-6 (b), under scanning electron microscope ABT55 (accelerating voltage 20 KV).

cially) concentrations to presence of accessory thorite or xenotime that is consistent with high Th concentration. In tectono-magmatic discrimination diagrams, data points characterizing the Nichatka complex plot predominantly in the field of syncollision granites (Fig. 4).

RESULTS OF U–Pb GEOCHRONOLOGICAL STUDY

We collected samples of the Kevakta and Nichatka granites for U–Pb geochronological analysis at the sites shown in Fig. 1. The results obtained are presented in Table 3 and illustrated in Figs. 5 and 6.

Granites of the Kevakta massif. Zircon fraction separated from biotite granite of the Kevakta massif (Sample L-384) mostly consists of idiomorphic to subidiomorphic transparent and translucent crystals of prismatic and long-prismatic zircon habit, which are colored pink to light lilac (Fig. 5). Main crystal faces are {100} and {110} of prism and {111}, {101} and {102} of dipyramid. Fine pores on uneven surface of crystals are likely the result of leaching. In single cases, pyramid apexes of zircon crystals are intensively colored dark lilac. In the inner crystal structure, there is distinguishable outer translucent semimetamict rim having low birefringence, representing sometimes about 50% of the crystal, and inner, more transparent unzoned core. In the outer rim, there are inclusions of biotite. Zircon crystals are from 30 to 250 μm in size; elongation coefficient from 1.5 to 2.5.

We used for isotopic analysis four fractions of most transparent and idiomorphic zircon grains (–85 + 60 and >150 μm; nos. 1–4, Table 3); zircon of two fractions was subjected to air-abrasion treatment that removed about 40 and 50% of substance (nos. 3 and 4, respectively; Table 3). Data points characterizing isotopic composition of studied zircons plot on discordia (Fig. 6) with upper intercept at 1846 ± 8 Ma and lower one at 387 ± 27 Ma (MSWD = 0.78). According to their morphology, zircons from granites of the Kevakta massif are of magmatic origin, and the estimated age of 1846 ± 8 Ma characterizes therefore the formation time of the massif.

Granites of the Nichatka complex. Accessory zircons separated from two-mica granites of the Nichatka complex (Sample 10263-6) are represented by subidiomorphic to idiomorphic cherry-colored transparent and translucent crystals of prismatic, short-prismatic and dipyramid habit (Fig. 5). Characteristic of crystals is combination of prism ({100} and {110}) and dipyramid ({111) and {112}) faces. Magmatic zoning is typical of their inner structure. Crystal cores are distinguishable in some translucent grains.

Isotopic data are obtained for three fractions of 2, 20 and 30 zircon crystals most transparent and idiomorphic (size fractions >150 and >100 μm). Crystals have been subjected to preliminary air-abrasion treatment

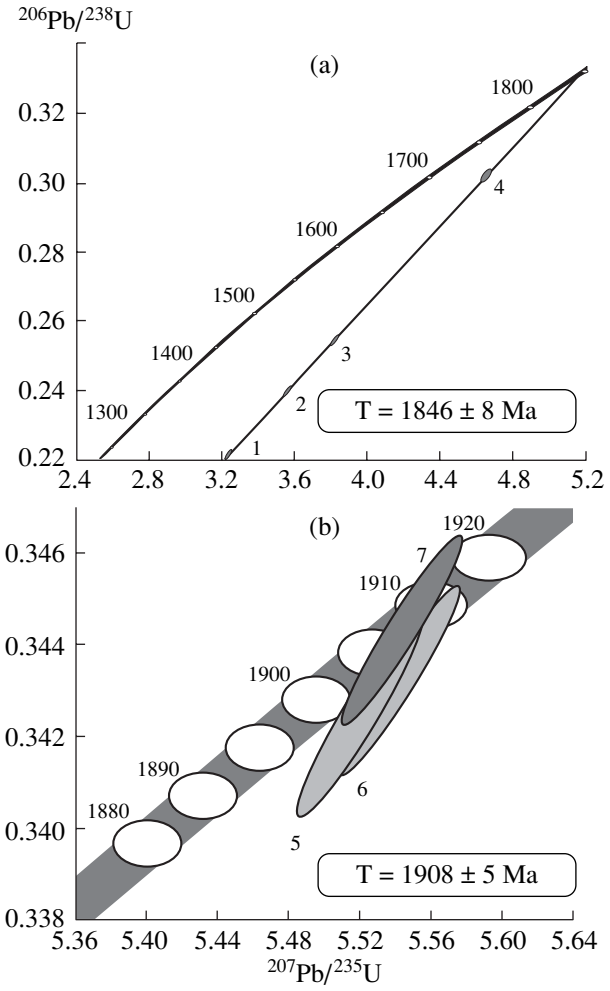

Fig. 6. Diagrams with concordia for zircons from granites of the Kevakta massif (a) and Nichatka complex (b); point numbers correspond to ordinal numbers in Table 3.

(nos. 5–7, Table 3). As one can see from Table 3 and Fig. 6, the data point characterizing one zircon residue after air-abrasion treatment (approximately a half of initial substance) is on concordia, while zircons of two other fractions are slightly discordant (discordance degree 0.5%). Age of concordant zircon is 1908 ± 5 Ma (MSWD = 0.004, concordance probability 0.95) that is very close to the $^{207}Pb/^{206}Pb$ age value of 1911 ± 7 Ma (MSWD = 4.2) characterizing in average three zircon fractions studied. According to morphological features, the analyzed zircons crystallized in magmatic melt, and the estimated age value of 1908 ± 5 Ma corresponds therefore to crystallization time of magma parental for granites of the Nichatka complex.

DISCUSSION

Geochronological results obtained show that granitoids of the Nichatka complex and Kevakta massif have been formed at different stages of the Early Proterozoic

Table 3. U-Pb isotopic characteristics of zircons from granitoids of the Kevakta massif and Nichatka complex

No.	Fraction size (μm) and characteristics	Weight, mg	Concentration, ppm		Isotopic ratios					Rho	Age, Ma		
			Pb	U	$^{206}Pb/^{204}Pb$	$^{207}Pb/^{206}Pb^{a}$	$^{208}Pb/^{206}Pb^{a}$	$^{207}Pb/^{235}U$	$^{206}Pb/^{238}U$		$^{207}Pb/^{235}U$	$^{206}Pb/^{238}U$	$^{207}Pb/^{206}Pb$
Granite of the Kevakta massif, Chuya–Kodar complex (Sample L-384)													
1	–85 + 60	0.79	64.9	279	2237	0.1061 ± 1	0.0879 ± 1	3.2382 ± 65	0.2213 ± 4	0.93	1466 ± 3	1289 ± 3	1734 ± 1
2	>150	0.61	36.0	113	299	0.1089 ± 1	0.1156 ± 1	3.8208 ± 76	0.2544 ± 5	0.89	1597 ± 3	1461 ± 3	1782 ± 1
3	–85 + 60, A 40%	0.43	32.8	125	852	0.1078 ± 1	0.0972 ± 1	3.5632 ± 71	0.2398 ± 5	0.91	1541 ± 3	1386 ± 3	1762 ± 1
4	>150, A 50%	0.46	77.6	148	106	0.1114 ± 1	0.1744 ± 1	4.6461 ± 88	0.3024 ± 6	0.76	1758 ± 4	1703 ± 3	1823 ± 2
Granite of the Nichatka complex (Sample 10263-6)													
5	>150, 2 grains, A 30%	–	U/Pb* 2.97		5260	0.1169 ± 1	0.0193 ± 1	5.5188 ± 110	0.3423 ± 7	0.94	1904 ± 4	1898 ± 4	1910 ± 1
6	>100, 20 grains, A 30%	–	U/Pb* 2.94		6255	0.1171 ± 1	0.0270 ± 1	5.5433 ± 111	0.3432 ± 7	0.96	1907 ± 4	1902 ± 4	1913 ± 1
7	>100, 30 grains, A 50%	0.15	67.2	193	1692	0.1168 ± 1	0.0337 ± 1	5.5443 ± 111	0.3443 ± 7	0.95	1908 ± 4	1907 ± 4	1908 ± 1

Notes: Isotopic ratios are corrected for blank and common lead; percentages after letter A denote amount of original substance removed by air-abrasion treatment; fractions marked by asterisk have not been weighted. The modified Krogh's method (Krogh, 1973) has been used to decompose crystals and to extract Pb and U. Isotopic composition is determined in static mode on multicollector mass spectrometer Finnigan MAT 261: uncertainty of U/Pb ratios corresponds to 0.5% and total blank was not greater than 0.1 ng for Pb and 0.005 ng for U. Air-abrasion treatment is performed using standard procedure (Krogh, 1982). Experimental data are processed using programs PbDAT and ISOPLOT (Ludwig, 1991; 1999). Standard U decay constants (Steiger and Jager, 1976) are used to calculate age values. Correction for common lead is consistent with model by Stacey and Kramers (1975). All uncertainties are quoted at 2σ level.

history of the Baikal fold area. It is also remarkable that granites of the Nichatka complex (1908 ± 5 Ma) are close in age to synkinematic granite-gneiss domes of the Cis-Olkhon region (1890 ± 25 Ma, Bibikova et al., 1990) and to event of granulite metamorphism in the Angara–Kan block (1900 ± 10 Ma, Bibikova et al., 1993). They are also comparable in age with gneissic granites of the Kuanda complex dated at 1895 ± 30 Ma (*Geological Structure…*, 1986). Fedorovskii (1985) regarded all these complexes as typical synmetamorphic interrelated granitoids. Gneissic granites of the Kuanda complex form numerous cupola-shaped massifs (diapir plutons) along flanks of the Kodar–Udokan trough, which originated under conditions of amphibolite metamorphic grade. In the northwestern part of the Chara–Olekma block of the Aldan shield, where the block is in contact with the Patom zone of the Baikal fold area, gneissic granites of the Kuanda complex are replaced by granites of the Nichatka complex, and the andalusite-sillimanite metamorphic zone is changed into the kyanite-sillimanite one (Fedorovskii, 1985). Granitoids of both complexes are intruded by postcollision rapakivi-like granites of the Kodar complex (1873–1876 Ma, Larin et al., 2000).

Geological and geochemical data evidence affiliation of granites of the Nichatka complex with syncollision granites, which originated most likely during the partial melting of ancient (Late Archean) crustal substance in response to thermal relaxation and/or exhumation of orogen in the course of isothermal decompression (Larin et al., 2003a). The complex has been formed apparently during collision of the Aldan continental plate with the Nechera terrane.

Time span between emplacement of syncollision granites of the Nichatka complex and typical postcollision granites of the Kodar complex or igneous complexes of the North Baikal volcano-plutonic belt (Larin et al., 2003b) is 40–30 m.y. long. The age interval like this between the syn- and postcollision granitoid magmatism is typical in general of other foldbelts (Dobretsov et al., 2001; Bonin et al., 1998; Väisänen et al., 2000). According to theoretical calculations (Lobkovskii et al., 2004), commencement of the orogenic stage proper with the relief uplift up to 3–5 km is delayed for 20–40 m.y., as a rule, relative to the initial collision stage; exactly this time span is necessary for injection, in a considerable volume, of the lower crust plastic material into the axial zone of orogen.

The obtained geochronological dates are consistent with the earlier idea that the Chuya granitoid complex is heterogeneous (Neymark et al., 1998). It is reasonable therefore to retain the former name only for granitoids of the Chuya Uplift (Chuya complex 2020 Ma old), which reveal geochemical characteristics of island-arc granitoids, and to discriminate the Chuya–Kodar complex of later granitoids, the Kevakta massif inclusive, which are confined to the Tonod Uplift. Based on age of the Kevakta massif, its tectonic position in the Baikal fold area, and geochemical parameters of relevant granites, which are comparable with characteristics of typical postcollision granites, the massif should be included into the South Siberian postcollision magmatic belt (1.88–1.84 Ga). This giant belts extends along the southwestern flank of Siberian platform from the Angara–Kan block in the west to the eastern margin of the Chara–Olekma block of the Aldan shield in the east (Didenko et al., 2003a; Larin et al., 2002, 2003b). A typical feature of postcollision magmatic belts is joint occurrence of A- and S-granites in association with rocks of high-K calc-alkaline, shoshonite–latite, and ultra-K magmatic series, which are enriched in incompatible elements and interrelated in origin with subcontinental lithospheric mantle subjected to metasomatism (Bonin et al., 1998). Besides, the high-temperature low-pressure (HT/LP) metamorphism of extension settings is typical of the belts under consideration (Buck, 1991; Väisänen et al., 2000).

Within the South Siberian magmatic belt, rock associations of shoshonite–latite series are widespread in the North Baikal volcano-plutonic belt (1869 ± 6 to 1854 ± 5 Ma), where felsic rocks correspond to A-type granites (Neymark et al., 1998; Larin et al., 2002, 2003b). The Kevakta massif, a typical representative of crustal S-type granites, is structurally related with this volcano-plutonic belt, being confined to its northeastern termination. In the western part of South Siberian magmatic belt (Sharyzhalgai, Biryusa and Angara–Kan blocks), dominant igneous associations correspond to postorogenic A-type granites, e.g., to rapakivi granites of the Primorskii complex, charnockites of the Shumikha and Tatarnik complexes, and granites of the Sayan and Tarak complexes, which have been formed between 1869 and 1837 Ma (Donskaya et al., 2002, 2003; Levitskii et al., 2002; Nozhkin et al., 2003; Didenko et al., 2003b). In the eastern termination of this belt, within the Chara–Olekma geoblock of the Aldan shield, there are known rapakivi-like granites of the Kodar complex, layered mafic-ultramafic plutons of the China complex (1830 ± 50 Ma, *Geological Structure…*, 1986), and dike swarm of ultra-K lamproites of the Khani complex (~1870 Ma, Bogatikov et al., 1991). Granulite metamorphism in the Sharyzhalgai block is dated at 1865 ± 5 Ma (Sal'nikova et al., 2003).

Since ~1.9 Ga ago, development of the South Siberian magmatic belt was interrelated with accretion of microplates, continental blocks and island arcs to the Siberian craton, and the belt stabilization culminated at ~1.8 Ga ago. Orogeny progressed from the east to the west (in present-day coordinates), and postcollision granitoids are getting younger from 1.87 to 1.84 Ga in the same direction (Sal'nikova et al., 2003) that is typical of transpression orogens. Thus, the South Siberian magmatic belt represents most likely a collision suture of the orogen. Origin of magmatic rock associations in the belt can be explained in terms of lithospheric delamination and extension collapse of overthickened

Table 4. Succession of Early Proterozoic tectonic events in the northern part of the Baikal fold area and western part of the Aldan shield

Northern part of the Baikal fold area	Chara–Olekma block of the Aldan shield
Postcollision tectonic events and magmatic complexes (South Siberian magmatic belt)	
1846 ± 8 Ma Chuya–Kodar complex of S-type K-granites (Kevakta massif)	
from 1854 ± 5 to 1869 ± 6 Ma North Baikal volcano-plutonic belt (igneous rocks of shoshonite and high- to medium-K calc-alkaline series, A-type granitoids)	
	from 1873 ± 2 to 1876 ± 4 Ma Kodar complex of rapakivi-like A-type granites
	1830 ± 50 Ma China complex of mafic-ultramafic layered plutons
	~1870 Ma Khani dike swarm of lamproites
Syncollision tectonic events and magmatic complexes	
1908 ± 4 Nichatka complex of high-Al S-type granites	
	1895 ± 30 Ma Kuanda complex of rheomorphic granites (diapir plutons)
	1895 ± 4 Ma Metamorphism of amphibolite grade and ultrametamorphism
Suprasubduction magmatism of magmatic arcs	
2020 ± 12 Ma Chuya complex of diorites, granodiorites and granites (M- and I-types)	
Formation of passive continental margin	
	2066 ± 6 Ma Katugin complex of alkaline granites
	>2.18 and <2.07 Ga Epicratonic basins of the Udokan type

crust, which took place 30–50 m.y. after the main collision event (Larin et al., 2002).

Consequently, the Early Proterozoic development history of the Baikal fold area and its junction zones with the Aldan shield and Dzhygdzhur–Stanovoi fold area (Table 4) lasted from emergence of island arcs 2020 Ma ago to the final stabilization 1850 Ma ago. It practically corresponds in duration to the formation period of the Early Proterozoic giant foldbelt of the Aldan shield (Kotov, 2003), being about 170 m.y. long and comparable with formation periods of similar structures in the other regions of the world (Kotov, 2003; Gaal and Gorbatschev, 1987).

CONCLUSIONS

Geochemical and geochronological data of this study show that Early Proterozoic granitoids of the Nichatka complex and Kevakta massif originated at different stages of geological evolution of the Baikal fold area and in different geodynamic settings. Origin of syncollision granites of the Nichatka complex dated at 1908 ± 5 Ma was interrelated with collision of the Aldan–Olekma microplate and Nechera terrane that caused thermal relaxation and/or exhumation of orogen in the course of isothermal decompression (Larin et al., 2003a).

Granites of the Kevakta massif definitely belong to the South Siberian postcollision magmatic belt. Since ~1.9 Ga, development of this belt was interrelated with successive accretion of microplates, continental blocks, and island arcs to the Siberian craton. These granites sharply differ in age and composition from granitoids of the Chuya complex they have been formerly attributed to. Accordingly, it is reasonable to divide the former association of granitoids into the Chuya complex proper of diorite–granodiorite association, which is ~2.02 Ga old, possessing geochemical characteristics of island-arc granitoids, and the Chuya–Kodar complex of postcollision S-type granitoids 1.85 Ga old.

In general, the Early Proterozoic development history of the Baikal fold area and its junction zone with the Aldan shield lasted about 170 m.y. In duration, it is comparable with formation periods of similar structures in the other regions of the world.

ACKNOWLEDGMENTS

The work was supported by the Russian Foundation for Basic Research, project nos. 03-05-64893, 04-05-64810, 06-05-64989, and by priority research programs "Isotopic geology: Geochronology, Substance Sources" and "Geodynamic Evolution of Lithosphere of Central Asian Mobile Belt (from Ocean to Continent)" of the Geoscience Division RAS and the Foundation for Encouragement of Domestic Science.

Reviewers M.G. Leonov, M.A. Semikhatov, and V.V. Yarmolyuk

REFERENCES

1. N. G. Berezhnaya, E. V. Bibikova, A. V. Sochava, et al., "isotopic Composition of the Chinei Subgroup of the Udokan Group, the Kodar–Udokan Trough," Dokl. Akad. Nauk SSSR **302** (5), 1209–1212 (1988).
2. E. V. Bibikova, T. I. Kirnozova, and V. A. Makarov, *Precambrian Geology and Geochronology of Siberian Platform and Flanking Structures* (Nauka, Leningrad, 1990), pp. 162–170 [in Russian].
3. E. V. Bibikova, T. V. Gracheva, V. A. Makarov, and A. D. Nozhkin, "The Age Boundaries of the Early Precambrian Geological Evolution of the Yenisei Ridge," Stratigr. Geol. Korrelyatsiya **1** (1), 35–40 (1993) [Stratigr. Geol. Correlation **1** (1), 29–35 (1993)].
4. O. A. Bogatikov, I. D. Ryabchikov, V. A. Kononova, et al., *Lamproites* (Nauka, Moscow, 1991) [in Russian].
5. B. Bonin, A. Azzuni-Sekkal, F. Bussy, and S. Ferrag, "Alkali-Calcic and Alkaline Post-Orogenic (PO) Granite Magmatism: Petrologic Constraints and Geodynamic Settings," Lithos. **45**, 45–70 (1998).
6. W. R. Buck. "Models of Continental Lithospheric Extension," J. Geophys. Res. **96**, 20161–20178 (1991).
7. A. N. Didenko, I. K. Kozakov, E. V. Bibikova, et al., "Paleoproterozoic Granites of the Sharyzhalgai Block, Siberian Craton: Paleomagnetism and Geodynamic Inferences," Dokl. Akad. Nauk **390** (3), 368–373 (2003a) [Dokl. Earth Sciences **390** (4), 510–515 (2003a)].
8. A. N. Didenko, V. Yu. Vodovozov, I. K. Kozakov, et al., "Methodological Aspects of Combined Paleomagnetic and Geochronological Study of Early Proterozoic Post-Collision Granitoids in the South of Siberian Craton," in "Proc. of the Second Russian Conference on Isotopic Geology: Isotopic Geochronology in Solution of Problems of Geodynamics and Ore Formation, November 25–27, 2003, St. Petersburg (Tsentr Inform. Kul'tury, St. Petersburg, 2003), pp. 148–152 [in Russian].
9. N. L. Dobretsov, A. G. Kirdyashkin, and A. A. Kirdyashkin, *Endogenic Geodynamics, 2nd Edition* (GEO, Novosibirsk, 2001) [in Russian].
10. T. V. Donskaya, E. V. Bibikova, A. M. Mazukabzov, et al., "Primorskii Complex of Granitoids in the West Baikal Region: Geochronology, Geodynamic Typification," Geol. Geofiz. **44** (10), 1006–1016 (2003).
11. T. V. Donskaya, E. B. Sal'nikova, E. V. Sklyarov, et al., "Early Proterozoic Postcollision Magmatism at the Southern Flank of the Siberian Craton: New Geochronological Data and Geodynamic Implications," Dokl. Akad. Nauk **382** (5), 663–667 (2002) [Dokl. Earth Science **383** (2), 125–128 (2002)].
12. V. S. Fedorovskii, *Lower Proterozoic of the Baikal Mountains (Geology and Formation of Continental Crust)* (Nauka, Moscow, 1985) [in Russian].
13. B. R. Frost, R. J. Arculus, C.G. Barnes, et al., "A Geochemical Classification of Granitic Rock Suites," J. Petrol. **42**, 2033–2048 (2001).
14. G. Gaal and R. Gorbatschev, "An Outline of the Precambrian Evolution of the Baltic Shield," Precambrian Res. **35**, 15–52 (1987).
15. *Geology of the USSR and Distribution Patterns of Mineral Deposits. Vol. 7: Altai–Sayan and Transbaikal–Amur regions,* Ed. by V. A. Amantov (Nedra, Leningrad, 1986) [in Russian].
16. A. B. Kotov, Doctorial Dissertation in Geology and Mineralogy (St. Petersburg, 2003).
17. T. E. Krogh, "A Low-Contamination Method for Hydrothermal Decomposition of Zircon and Extraction of U and Pb for Isotopic Age Determination," Geochim. Cosmochim. Acta **37**, 485–494 (1973).
18. T. E. Krogh, "Improved Accuracy of U–Pb Zircon Dating by the Creation of More Concordant Systems Using an Air Abrasion Technique," Geochim. Cosmochim. Acta **46**, 637–649 (1982).
19. A. M. Larin, A. B. Kotov, S. B. Salnikova, and V.P. Kovach, "Late Paleoproterozoic Postcollisional and Anorogenic Volcanic Sequences of the Siberian Craton: Petrogenesis and Tectonic Implications," in *II Simposio: Vulcanismo e Ambientes Associados* (Belem-PA, Brasil, 2002), p. 18.
20. A. M. Larin, A. B. Kotov, E. B. Sal'nikova, et al., "New Data on the Age of Granites of the Kodar and Tukuringra Complexes, Eastern Siberia: Geodynamic Constraints," Petrologiya **8** (3), 267–279 (2000) [Petrology **8** (3), 238–248 (2000)].
21. A. M. Larin, A. B. Kotov, E. B. Sal'nikova, and V. P. Kovach, "Early Proterozoic Postcollision Belt in Southwestern Flank of Siberian Platform," in "Geology, Geochemistry and Geophysics by Transition from XX to XXI Century" (Svyaz'-print, Moscow, 2002), pp. 53–55 [in Russian].
22. A. M. Larin, L. A. Neymark, A. A. Nemchin, and E. Yu. Rytsk, "Two Different Types of Neoproterozoic Tin-Bearing Granites in the Baikal Mountain Region," in *Intern. Field Conference: Proterozoic Granite Systems of the Pennokean Terrane in Wisconsin*. (Madison, 1998), pp. 155–156.
23. A. M. Larin, E. B. Sal'nikova, A. B. Kotov, et al., "North Baikal Volcano-Plutonic Belt: Age, Formation Period and Tectonic Position," Dokl. Akad. Nauk **392** (4), 506–511 (2003a) [Dokl. Earth Science **392** (7), 392–397 (2003a)].
24. A. M. Larin, E. B. Sal'nikova, A. B. Kotov, et al., "Age and Geodynamic Typification of Early Proterozoic Granitoids in the Baikal Fold Area," in *Proc. of the Second Russian Conference on Isotopic Geology: Isotopic Geochronology in Solution of Problems of Geodynamics and Ore Formation, November 25–27, 2003, St. Petersburg* (Tsentr Inform. Kul'tury, St. Petersburg, 2003b), pp. 249–252 [in Russian].

25. V. I. Levitskii, A. I. Mel'nikov, L. Z. Reznitskii, et al., "Post-Kinematic Early Proterozoic Granitoids in the Southwest of Siberian Platform: Geochronology, Geodynamic Typification," Geol. Geofiz. **43** (8), 717–732 (2002).

26. L. I. Lobkovskii, A. M. Nikishin, and V. E. Khain, *Current Problems of Geotectonics and Geodynamics* (Nauchnyi Mir, Moscow, 2004) [in Russian].

27. K. R. Ludwig, "PbDAT for MS-DOS, Version 1.21," U.S. Geol. Survey Open-File Rep., No. 88-542, 1–35 (1991b).

28. K. R. Ludwig, "ISOPLOT/Ex. Version 2.06. A Geochronological Toolkit for Microsoft Excel," Berkley Geochronology Center Sp. Publ., No. 1a, 1–49 (1999).

29. L. A. Neymark, A. M. Larin, A. A. Nemchin, et al., "Anorogenic Nature of Magmatism in the North Baikal Volcanic Belt: Evidence from Geochemical, Geochronological (U–Pb), and Isotopic (Pb, Nd) Data," Petrologiya **6** (2), 139–164 (1998) [Petrology **6** (2), 124–148 (1998)].

30. A. D. Nozhkin, E. V. Bibikova, O. M. Turkina, and V. A. Ponomarchuk, "Isotopic-Geochronological Investigations (U–Pb, Ar–Ar, Sm–Nd) of Subalkaline Porphyroid Granites, the Tarak Massif of the Yenisei Ridge," Geol. Geofiz. **44** (9), 879–889 (2003).

31. J. A. Pearce, N. B. W. Harris, and A. G. Tindle, "Trace Element Distribution Diagrams for the Tectonic Interpretation of Granitic Rocks," J. Petrol. **25** (4), 956–983 (1984).

32. J. A. Pearce, "Sources and Setting of Granitic Rocks," Episodes **19** (4), 120–125 (1996).

33. E. B. Sal'nikova, A. B. Kotov, V. I. Levitskii, et al., "Age Boundaries of High-Temperature Metamorphism in Crystalline Complexes of Sharyzhalgai Basement Rise in Siberian Platform: U–Pb Dating of Individual Zircon Grains," in *Proc. of the Second Russian Conference on Isotopic Geology: Isotopic Geochronology in Solution of Problems of Geodynamics and Ore Formation, November 25–27, 2003, St. Petersburg* (Tsentr Inform. Kul'tury, St. Petersburg, 2003), pp. 453–455 [in Russian].

34. J. S. Stacey and I. D. Kramers, "Approximation of Terrestrial Lead Isotope Evolution by a Two-Stage Model," Earth Planet. Sci. Lett. **26** (2), 207–221 (1975).

35. R. H. Steiger and E Jager, "Subcommission of Geochronology: Convention of the Use of Decay Constants in Geo- and Cosmochronology," Earth Planet. Sci. Lett. **36** (2), 359–362 (1976).

36. S. R. Taylor and S. M. McLennan, *The Continental Crust: Its Composition and Evolution* (Blackwell, Oxford, 1985; Mir, Moscow, 1988).

37. M. Väisänen, I. Mänttäri, L. M. Kriegsman, and P. Hölttä, "Tectonic Setting of Post-Collisional Magmatism in the Palaeproterozoic Svecofennian Orogen, SW Finland," Lithos **54**, 63–81 (2000).